



1 **Proposed improvement of the detection and measurements of**
2 **light precipitation in the Canadian Arctic**
3

4 Joseph Durat^{1,2}, Hadleigh D. Thompson², Julie M. Thériault², Philip Marsh³
5

6 ¹UFR PhITEM, Université Grenoble Alpes, 38400, Saint-Martin-d'Hères, France

7 ² Department of Earth and Atmospheric Sciences, Centre ESCER, Université du Québec à Montréal, Montréal,
8 Quebec, H3C 3P8, Canada

9 ³Cold Regions Research Centre, Wilfrid Laurier University, Waterloo, Ontario, Canada

10

11 *Corresponding author:* Julie M. Thériault (theriault.julie@uqam.ca)



12 **Abstract.** Snowfall during the extended cold season experienced in Arctic regions is the primary contributor to
13 snowpack evolution, terrestrial components of the water cycle, and many melt-season hydrologic phenomena.
14 Despite this importance, solid precipitation measurements in the Arctic are challenging; frequent periods of light
15 precipitation are often difficult to measure with existing gauge networks, and result in under-estimations of total
16 snowfall during a winter season. This study analyzes the measurement of solid precipitation at the Trail Valley
17 Creek Research Station in the Canadian Northwest Territories, using a weighing precipitation gauge, and micro
18 rain radar. The study period runs from 4 November 2023 to 30 April 2024, with an intensive observation period
19 from 16 March to 2 April 2024, during which detailed manual observations improved our understanding of
20 instrument performance in arctic conditions. The already established weighing gauge was used as the reference
21 for the study and measured a total snowfall (snow water equivalent) during the study period of 68 mm, which
22 increased to 190 mm after corrections for wind and snowfall intensity. Manual observations coupled with radar,
23 however, confirm the difficulty of measuring light precipitation. We present a method of on-site calibration for
24 the reflectivity-snowfall relationship for the micro rain radar, that we use to estimate the low-rate ($< 0.2 \text{ mm hr}^{-1}$)
25 snowfall amounts that are commonly missed by weighing gauges. Adding these trace amounts of precipitation, the
26 total snowfall amount increased by another 24%. While more work is required to confirm these methods in Arctic
27 environments, this study contributes to a better understanding of current measurement systems and can be used to
28 enhance snowfall estimations.



29 **1 Introduction**

30 The high-latitude regions of the world are of great interest in the context of climate change, however, they are
31 poorly understood and surveyed due to their remote location and harsh climate (Brunet and Milbrandt, 2023,
32 Souverijns et al., 2017). These areas are also the most impacted by global warming, with effects such as enhanced
33 changes in near-surface air temperature being observed due to arctic amplification (Previdi et al., 2021). Snow in
34 the Arctic plays a major role in the local permafrost and hydrology, and in regional and global energy balances
35 (Marsh and Pomeroy, 1996; Chen et al., 2021; O'Neill and Burn, 2017). Total snowfall measurement, however, is
36 challenging; with end of winter snow on the ground often being larger than measured snowfall (Woo et all, 1983).
37 Such errors are due to frequent periods of trace amounts of snow being often difficult to measure, with many
38 existing gauge networks having a minimum detectable precipitation rate higher than what has been observed in
39 polar regions (Colli and Rasmussen, 2015; Gultepe et al., 2016, Matrosov et al., 2022, Mariani et al., 2024). These
40 periods of light precipitation (rates from 0.1 to 0.5 mm hr⁻¹, depending on the study), can be missed by conventional
41 gauges designed for mid and low latitudes. Light precipitation can nonetheless significantly contribute to the
42 snowpack throughout the winter, representing 80% of the precipitation over arctic regions in terms of duration,
43 and up to 45 to 50% in terms of amount (Gultepe et al., 2016, Matrosov et al., 2022).
44 Depending on the type of hydrometeor, wind speed, and gauge design, many precipitation gauges have
45 shortcomings when measuring snowfall rate and amount (Rasmussen et al., 2012, Mariani et al., 2024).
46 Underestimated snowfall can be adjusted using transfer functions that include wind speed, temperature, particle
47 fall speed (Leroux et al., 2021), and snow intensity (Colli et al., 2020). Even with such adjustments, the total
48 precipitation measured by a weighing precipitation gauge with a single-Alter windshield may be incorrect by as
49 much as 54% to 123% when compared to a Double Fence Automated Reference (DFAR), (Smith et al., 2020).
50 More advanced instruments, such as laser and video disdrometers and hotplate precipitation gauges have been
51 developed to address some of the shortcomings of weighing precipitation gauges, and to enhance analysis of
52 precipitation characteristics (see Leroux et al., 2021; Thériault et al., 2021). Challenges such as access to reliable
53 AC power, data storage and recovery, and accuracy in harsh environments, remain. Optical disdrometers, for
54 example, are known to have issues characterizing the precipitation rate during periods of snow due to border
55 effects, one-dimensional size characterization of particles, and shadow effect for simultaneous particles (Battaglia
56 et al., 2010; Kochendorfer et al., 2022).
57 Experimentation to retrieve solid precipitation measurements in polar regions has recently evolved with the use of
58 vertically pointing radars. Beyond identifying precipitation formation processes aloft, techniques have been
59 developed to retrieve snowfall rates (Matrosov et al., 2022). Schoger et al. (2021), and Souverijns et al. (2017),
60 both used micro rain radars (MRRs) in Svalbard Norway, and Princess Elizabeth, Antarctica, respectively, in
61 combination with W-band cloud radars and optical disdrometers. Using the relationship between radar reflectivity
62 and snowfall rate removes the necessity to catch and weigh precipitation or rely on particles being intercepted
63 within a small footprint at the surface. Snowfall studies in Antarctica differ from this research however, due to the
64 small number of large snowfall events across the southern hemisphere continent that are driven by large-scale
65 process such as atmospheric rivers (Gorodetskaya et al., 2014, as cited in Souverijns et al., 2016). To enrich
66 meteorological measurements in the Canadian arctic, two federally funded supersites have been established in
67 Whitehorse and Iqaluit, which make use of an array of radar, lidar, and remote sensing instrumentation (Mariani
68 et al., 2022; also see Mariani et al., 2024). These instruments are primarily used to support operational forecasting



69 and numerical weather prediction models, and both sites are located near population centers and upper air
70 observations stations. Neither site currently has an MRR in operation.

71 For this study, an established meteorological station at a high-latitude site in the western Canadian Arctic, Trail
72 Valley Creek Research Station (TVC), was supplemented with an optical disdrometer, MRR, and hotplate for the
73 2023-2024 winter. Accompanying manual observations were made during March-April 2024. The catchment hosts
74 an assortment of hydrological research activities that began in 1991 (Marsh et al., 2004), with recent studies
75 ranging from the water balance of thermokast lakes (Wilcox et al., 2023), to tundra snowpack modelling (Meloche
76 et al., 2022). Outside the catchment, research includes studies of the region's biodiversity, hydrological regimes
77 (Morse et al., 2012), and permafrost (O'Neill and Burn, 2017). Difficulties in the closure of catchment water
78 balances, however, are exacerbated when total winter snowfall amounts are at best underestimated where measured
79 and missing where data are sparse. While snow surveys are carried out each spring in the catchment to record total
80 snow depth and snow water equivalent (SWE) on the ground, it is the accurate measurement of snowfall throughout
81 the winter that remains a challenge at TVC.

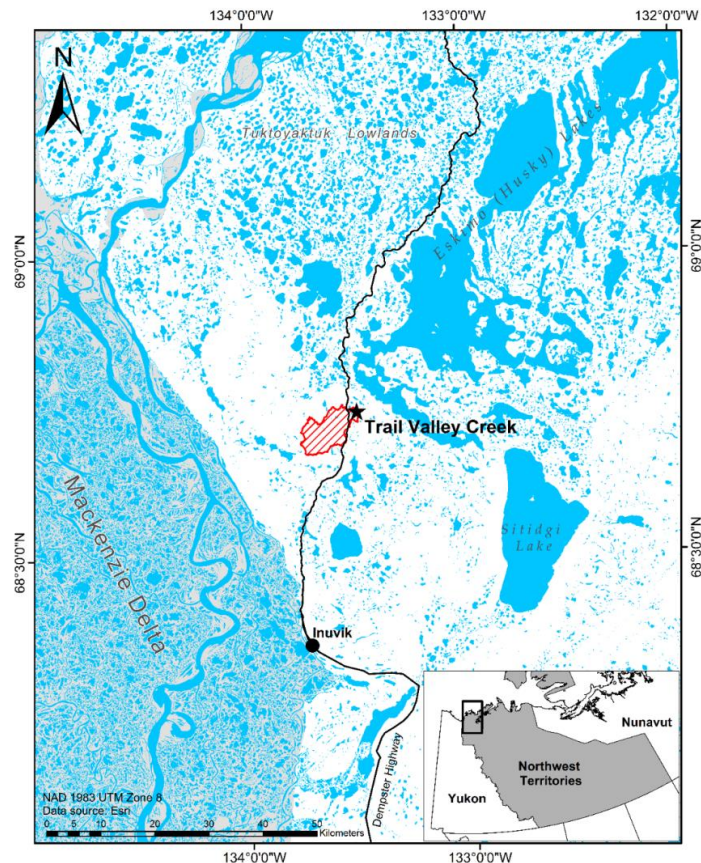
82 Accordingly, the goal of this study is to propose a method to improve the estimation of light precipitation. To do
83 so, we use a combination of in situ measurements from the federally operated weighing precipitation gauge, the
84 MRR, and manual observations. Technical issues and reliable power for the disdrometer and hotplate prevent us
85 from utilizing data from these instruments during the study period.

86 The manuscript is organized as follows: Section **Error! Reference source not found.** details the site, instruments,
87 and methods used in the study, and in Section 3 we present the results of the 2023 – 2024 data collected at TVC.
88 In Section 4 we discuss the results, the reliability of the instruments in the Canadian Arctic, the performances of
89 various corrections, and the added value of the intensive observation period. Section 5 provides a summary and
90 conclusions.

91 **2. Methods**

92 **2.1 The study site**

93 Trail Valley Creek Research Station (TVC) (68°44'31.2"N, 133°29'55.3"W) (Fig.1), first established in 1991, lies
94 50 km north of Inuvik, Northwest Territories, and ~75 km south of the Arctic Ocean coastline. It is a continental
95 location with a subarctic climate, and Inuvik climatology from 1965 to 1995 indicates a mean annual precipitation
96 of ~340 mm, with ~207 mm being snow (Environment and Climate Change Canada, 2023). Marsh et al. (2010)
97 described long term changes in snowfall at Inuvik and at TVC. Precipitation trends in the region, however, have
98 been positively correlated with the warming of the Arctic in recent years (Przybylak, 2002).



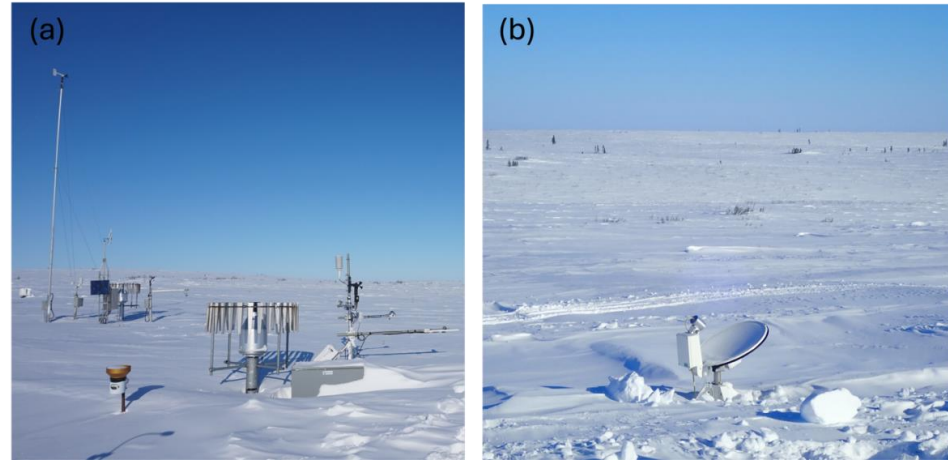
99

100 **Figure 1. Trail Valley Creek and northwestern Northwest Territories.** Shown is the Mackenzie Delta, the town of Inuvik
101 (center bottom), and the Dempster and Inuvik to Tuktoyaktuk highways (black line). Also displayed is the weather
102 station used in this study (black star), and the Trail Valley Creek watershed (red polygon) (adapted from Walker and
103 Marsh, (2019)).

104 The station operates on solar power and battery for as much of the arctic summer as possible, with a backup
105 generator charging the battery bank at all other times. The selection of instrumentation therefore is limited as
106 power consumption is a continuous concern. Regardless of this, the station manages a broad array of
107 hydrometeorological instruments and camp facilities, considering it is 5 and 8 degrees north of the federally funded
108 supersites in Iqaluit and Whitehorse, respectively. The instruments used in this study are shown in Fig. 2.



109



110
111
112
113
114

Figure 2: Instruments used at Trail valley Creek. (a) The Environment and Climate Change Canada 10 m mast, Geonor weighing precipitation gauge (furthest gauge to the left), and temperature, pressure, and humidity sensors. In the foreground, Wilfrid Laurier University instruments with another Geonor, anemometer, radiometer, and a snow depth sensor. Only data from the ECCC instruments were used in this analysis. (b) The METEK micro rain radar MRR2. All images taken April 2024, with snowpack depth being near the seasonal maximum for the 2023 – 2024 winter.

115

2.2 Instruments and data

116
117
118
119
120
121
122
123
124

The Environment and Climate Change Canada (ECCC) station at TVC (Climate ID: 220N005; WMO ID: 71683) comprises a Geonor weighing precipitation gauge with single Alter wind shield (henceforth referred to as the Geonor), a 10 m mast with an RM Young wind monitor, and pressure, temperature, and humidity sensors (Fig. 2a). Hourly data are available from 1998, making it a valuable resource in this data-sparse region. Data for this study were downloaded from November 2023 to May 2024 from ECCC's historical data website. A similarly instrumented weather station operated by Wilfrid Laurier University (WLU) is collocated with the ECCC station, however, the WLU instruments are configured for research purposes, as opposed to the operational ECCC station. Hourly ECCC data is also the typical resource the wider hydrometeorological community uses for precipitation measurements in the area.

125
126
127
128
129

The ECCC Geonor is equipped with a single alter shield to decrease wind-induced precipitation undercatch; however, even with this shield this gauge is known to still under estimate solid precipitation (Leroux et al., 2021). As a result of multiple studies (e.g., Kochendorfer et al. 2017, 2018; Pierre et al. 2019), several collection efficiency (CE) equations have been developed using different meteorological parameters. The measured precipitation rate ($P_{measured}$) can then be adjusted ($P_{adjusted}$) using CE with:

$$P_{adjusted} = \frac{P_{measured}}{CE} \quad (1)$$

130
131

Despite having a disdrometer, there were too many data gaps to use methods developed in Leroux et al. (2021); therefore we use in this study the transfer function developed by Colli et al. (2020) referred to as $f_{(U, SI)}$, using:

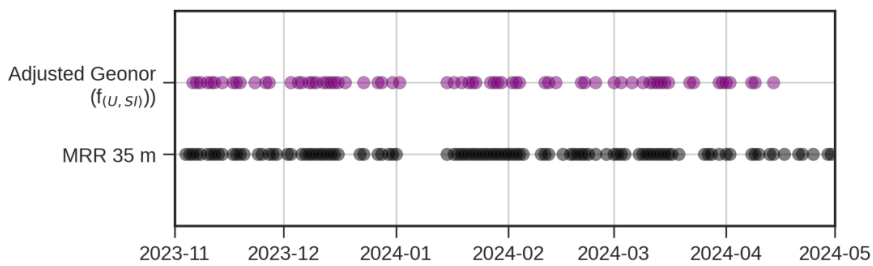
$$CE = e^{a(U_w)(1 - [tan^{-1}(b(SI) + c)])} \quad (2)$$

132
133
134

With U_w the wind speed at 2-m height and SI the unadjusted snowfall intensity (SI) in $mm\ h^{-1}$ from a single-Alter Geonor gauge. Equation 1 is based on data collected at Marshall in Colorado, Centre for Atmospheric Research Experiments in Canada (CARE), and Haukelister in Norway from fall 2013 to spring 2015. Each site has different



135 weather conditions and therefore uses different coefficients. We use coefficients from the Marshall measurement
136 site ($a = 0.4156$, $b = 8.7795$, and $c = -0.7062$). Similarly to Colli et al., (2020), we use wind speed measured at 10
137 m height (U) and employ adjustment $U_w = 0.71 * U$ to obtain the 2 m wind speed. We limit the maximum wind
138 speed to 10 m s^{-1} (Colli et al., 2020).
139 Regardless of the transfer function used, adjustments to precipitation amounts can only be performed when the
140 hourly values are greater than zero. Configurations for Geonor (and similar) gauges vary depending on the location
141 and network. For the Geonor located at TVC, the minimum measurement threshold was set to 0.2 mm per hour.



142
143 **Figure 3.** Time series (daily resolution) of snowfall signals recorded at Trail Valley Creek Research Station by the
144 Geonor weighing precipitation gauge (purple circles), and the METEK MRR2 (black circles).

145 **2.3 Micro rain radar**

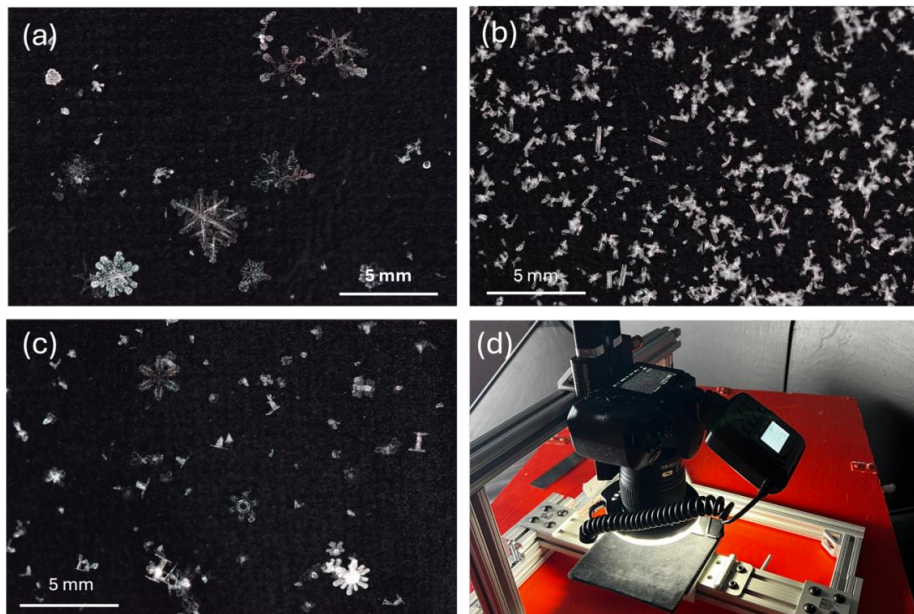
146 The MRR (Fig. 2b) is a vertically orientated, continuously transmitting, 24 GHz meteorological radar using a 2°
147 wide beam reflected from a ~ 70 cm parabolic dish. The dish is heated to avoid snow and ice buildup during
148 precipitation events. The resulting data include information on particle reflectivity and the vertical velocity of
149 hydrometeors aloft (Metek, 2009). The 32 range gates can be set to a vertical resolution between 35 m and 200 m.
150 To capture the greatest range, we employed a novel method of switching between 35 m and 200 m vertical
151 resolutions every ~ 30 seconds using a function in the manufacturer-supplied software. This allowed for the finer
152 details of near-surface precipitation to be observed, down to 70 m above ground level, while maintaining an
153 understanding of the mid-level source of the precipitation particles (i.e., most cloud tops are above the 1120 m
154 maximum height observed when using only the 35 m resolution). Data from both resolutions were post-processed
155 using Maahn and Kollias, (2012), which increases the instrument's sensitivity to light solid precipitation (Thériault
156 et al., 2021). The timing of precipitation detected from the MRR agrees well with the Geonor precipitation gauge
157 (Fig. 3), a benefit of the instrument being located on a (relatively) reliable electrical circuit.

158 **2.4 Intensive observation period**

159 An Intensive Observation Period (IOP) took place from 2300 UTC 16 March until 1700 UTC 2 April 2024, and
160 followed the same structure described in Thériault et al. (2019) and Thompson et al. (2023). The aim of the IOP
161 in this study was to confirm the atmospheric conditions during periods of light precipitation and blowing snow,
162 and to evaluate instrument performance during these events. This also removed some of the guesswork when
163 analysing data after the field campaign. While the IOP was relatively short, conditions during the polar winter at
164 TVC prevent any substantial observation period earlier than March each year. During the IOP, weather
165 observations were taken every hour indicating either no precipitation, light precipitation, snow event, or blowing



166 snow event (or a combination of conditions). Sky conditions were also reported, as well as the primary and
167 secondary particle types in cases of precipitation.
168 An ice-fishing tent was installed to provide shelter for photography equipment in the hope of replicating the
169 macrophotography protocol used in previous mid-latitude experiments (e.g., Thériault et al., 2019) (Fig. 4).
170 Sporadic snowfall and low precipitation rates, however, prevented the routine photography of hydrometeors every
171 10-minutes as the collection pad was often not sufficiently covered with particles. This did provide an opportunity
172 for the field participants to delineate between *snow* and *light precipitation* in their observations: if the collection
173 pad was covered enough for a series of images to be taken then the precipitation type for the 10-minute period was
174 classed as snow; if snow or ice crystals were present but there were not enough hydrometeors on the pad to
175 photograph, then the precipitation type was classed as light precipitation. This method became more reliable than
176 using a snow board to estimate trace amounts of snow, as the board was usually stripped bare of snow by wind.
177 All observations used World Meteorological Organization standards (e.g., WMO, (2021)). The observations do
178 not cover most of local nighttime nor the period from 1700 UTC 26 March to 0300 UTC 28 March due to a
179 resupply trip to Inuvik.



180
181 **Figure 4. Macrophotographs and the photography equipment used during the intensive observation period (IOP).** (a)
182 taken on 30 March 2024, contains a collection of dendrites between 3-5 mm in size; (b) and (c) taken on 1 April 2024 ~2
183 hours apart, shows the transition of snow crystal type from columns, bullets, and ice particles ~1-2 mm in size, to capped
184 columns, plates, and dendrites 2-4 mm in size.

185 **2.5 Z-S estimation reflectivity**

186 Using the manual observations, a Z-S relationship was derived to determine the occurrence of light precipitation.
187 Snowfall (S) amount at the surface is related to the MRR reflectivity (Z_e) using:

$$S = \left(\frac{1}{a_{zs}} Z_e \right)^{1/b_{zs}} \quad (3)$$



188 with Z_e the effective reflectivity of the MRR, a_{zs} the prefactor, and b_{zs} the exponent value. We follow methods
189 used by Schoger et al. (2021) by taking the average backscattered signal Z_e every five minutes for the heights 105
190 m, 140 m, and 175 m, using the 35 m resolution data. There were no days of missing data during the study period;
191 however, the post-processing algorithm can struggle to dealiase all 10 second data, depending on noise in the
192 signal, which leads to the 5-minute averaging.

193 The range of values for a_{zs} and b_{zs} from previous studies highlights the complexity of the S-Ze relationship, which
194 is a function of particle size and shape, liquid water content, and precipitation type, in addition to other
195 environmental and microphysical properties. Despite previous studies warning against using a fixed climatological
196 S-Ze relationship (e.g., Rasmussen et al., 2003), and improvements being made using variable a_{zs} values, in this
197 study we are constrained to a fixed S-Ze relationship due to the mismatch in temporal resolution between the MRR
198 (1-minute) and Geonor (hourly), which is a situation we envision other hydrometeorological groups may
199 encounter. An attempt was made to replicate methods used by Rasmussen et al. (2003) and Schoger et al. (2021)
200 using data from the disdrometer; however, our dataset appears to be too noisy to obtain accurate estimates for b_{zs}
201 and a_{zs} . Values for b_{zs} for example, were a magnitude larger than expected (Rasmussen et al., 2003) and therefore
202 unphysical. We suspect this is due to very low rates of snowfall, yet high number of small particles observed (i.e.
203 below the size range of the disdrometer). To select the appropriate coefficients to use in this study, we first use the
204 average values from Schoger et al. (2021) ($a_{zs} = 77.61$, $b_{zs} = 1.22$), however this resulted in a gross underestimation
205 (~50%) of total snow accumulation compared to the adjusted Geonor values during the season. Conversely, using
206 Souverijns et al. (2017) ($a_{zs} = 18$, $b_{zs} = 1.10$), overestimated snow accumulation by a factor of 2. Taking these
207 bounds into consideration, we conducted a linear regression analysis that iterated Eq. (3) 10,000 times with
208 incremental steps for a_{zs} between 10 to 100, and b_{zs} between 1.0 and 2.0, using 206 hours of concurrent
209 measurements between the MRR and Geonor. From this, the linear regression model with the lowest RMSE and
210 closest total seasonal precipitation amount provided coefficients for Eq. (3) of $a_{zs} = 64.55$, $b_{zs} = 1.72$.

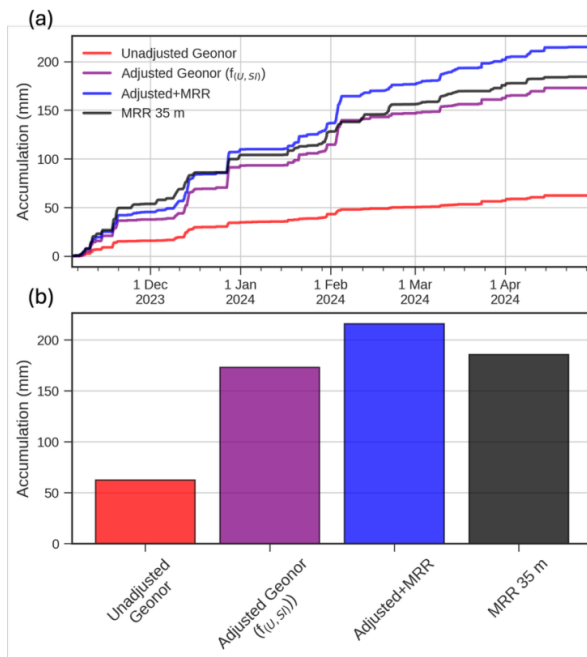
211 **3. Total accumulated precipitation: November 2023 – April 2024**

212 We constrain our analysis to data obtained from 4 November 2023 to 30 April 2024, when all instruments were
213 installed and configured as described in Section 2. TVC does experience snowfall outside of these months,
214 therefore total accumulation mentioned here does not represent total seasonal snow-on-the-ground at the site.
215 Additionally, we maintain the native resolution of the MRR in our analysis as the higher frequency of
216 measurements is a key feature in the increased sensitivity of these instruments to snowfall in this experiment. For
217 direct comparisons to the Geonor, we have accumulated the individual 1- or 5-minute precipitation amounts to
218 obtain hourly accumulation. We make these hourly comparisons sparingly, however, due to suspected dumps of
219 snow into the Geonor from capping (a build-up on snow and/or ice on the instrument housing) that resulted in the
220 timing of accumulation appearing to be misaligned.

221 During the study the temperature remained below 0°C during all episodes of precipitation, and only solid
222 precipitation was observed. The Geonor observed a total of 246 hours (Fig. 3) with 0.2 mm or more of precipitation,
223 with a maximum hourly amount of 2.0 mm (unadjusted) observed on 23 March 2024, and a daily maximum of 4.5
224 mm (unadjusted) on 18 November 2023. Of the 71 days during the study period that precipitation was observed
225 by the Geonor, 49 of those days had < 1 mm (unadjusted) of total accumulation (Fig. 4). The total unadjusted
226 accumulation for the study period from the Geonor was 62.3 mm (Figure 5), with ~50% of the total accumulation



227 falling in November and December 2023 (not shown). Adjusting the Geonor data using $f_{U,SI}$ (Eq. (3)), the total
228 observed accumulation increases 276% to 172 mm, with hourly accumulations increasing between 6.9% and
229 1409%, and the maximum daily accumulation becoming 28 mm on 27 December 2023.
230 The Geonor data exhibit a discontinuity at the lower ends of both the hourly and daily accumulation distributions,
231 i.e., no values below 0.2 mm (not shown); a fact that is exacerbated at this Arctic site due to the high frequency of
232 low-rate precipitation events during the study period. The Geonor therefore underestimates precipitation not only
233 due to gauge under catch, but also due to instrument sensitivity more so in the arctic than in the mid-latitudes.



234
235 **Figure 5.** Total precipitation accumulation for instruments and adjustments used in this study. (a) The time series from
236 237 4 November 2023 to 30 April 2024 for each instrument, and (b) total cumulative accumulation. Colors represent the
238 239 Unadjusted Geonor accumulation (red), adjusted Geonor accumulation, $f_{U, SI}$, using Colli et al. (2020) (purple);
Geonor-MRR adjusted (adjusted Geonor amount with additional MRR detected accumulation, see Section 3.3) (blue);
total accumulation using the MRR signal and Eq. (3) (black).

240 Summing the 5-minute precipitation amounts from the MRR data using Eq. (3) resulted in a total accumulation of
241 185 mm. The instrument detected precipitation for 1188 hours, with 5-minute average reflectivity ranging from
242 0.0678 dBz to 408.5 dBz, which equates to precipitation rates ranging from 0.018 to 2.92 mm hr⁻¹. This is in line
243 with the minimum threshold of 0.01 mm hr⁻¹ stated by Mahn and Kollas (2012). The daily maximum MRR
244 accumulation of 11.5 mm was recorded on 27 December 2023 (correlating with the Geonor).
245 Differences in the total accumulations between the MRR and the Geonor are primarily explained by the choice of
246 azs and bzs in Eq. (2), and the fact that they are not explicitly defined for TVC and this study. Regardless, the
247 amount measured by the MRR is a realistic first-order estimation. Other sources of error include sublimation of
248 particles between the measurement heights aloft and the surface, and horizontal transport of hydrometeors away
249 from the MRR location after the reflectively measurements were made. It would also be conceivable for the MRR
250 total to be greater than the Geonor due to the MRR method being immune to issues associated with weighing



251 gauges such as wind undercatch, instrument capping, and sublimation; problems that were noted by both Schogger
252 et al. (2021) and von Lerber et al. (2017) but that were not accounted for.

253 **4. Intensive Observation Period: March – April 2024**

254 Weather conditions during the IOP from 16 March 2024 to 4 April 2024 are shown in Figure 6. During this period,
255 the hourly manual observations comprised of 9 snow, 19 light precipitation, and 32 blowing snow observations.
256 There were 158 hourly observations of no precipitation (Table 1). The minimum and maximum temperatures
257 recorded during the IOP were -38°C and -3°C, respectively. (Fig. 6).

258

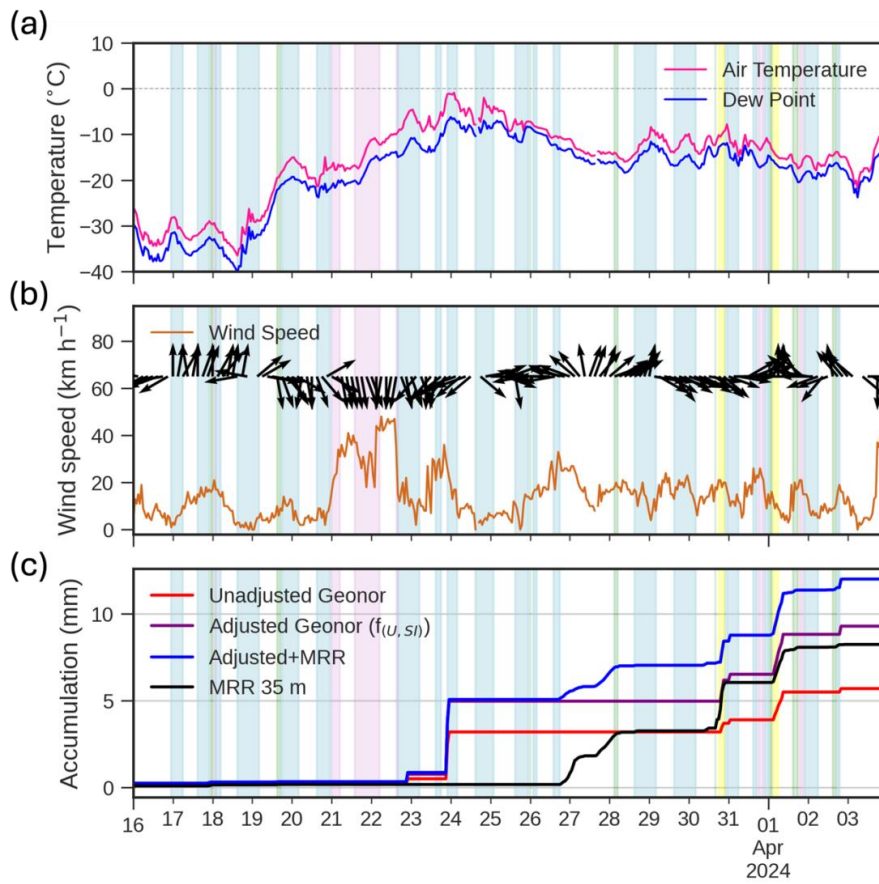
259 **Table 1. Instrument performance during the Intensive observation period hourly observations**

Instrument	Snow	Light precipitation	Blowing snow
Observed	9	19	32
Geonor	5	0	0
MRR	9	13	1

260

261 The Geonor recorded at least 0.2 mm precipitation for 5 of the 9 hours of snow (**Error! Reference source not**
262 **found.**), but none of the light precipitation or blowing snow observations. Precipitation rates from the MRR signal
263 could be calculated during the 9 hours of snow, one hour of blowing snow, and during 13 of the 19 hours of light
264 precipitation. For the 4 hours of snow that the Geonor failed to detect precipitation, the MRR data indicates
265 precipitation rates < 0.2 mm hr⁻¹. Notably, the Geonor recorded the maximum hourly accumulation during the
266 IOP on 23 March 2024 (2 mm). The manual observations and MRR signal indicate no precipitation occurring
267 during that time; however, warming (> 1°C hr⁻¹) at the surface towards 0.0°C for several hours preceding the
268 measurement suggests a dump from capping (a build-up on snow and/or ice) of the instrument housing.
269 Furthermore, sublimation of snow from inside the housing is not considered in this study but could play a minor
270 role in underestimating total accumulation.

271 From the IOP observations, we confirm there are frequent small amounts (< 0.2 mm) of precipitation at the surface
272 without being detected by conventional precipitation gauges. From here, we propose a method to quantify these
273 amounts and analyse their contribution to seasonal snow totals at Trail Valley Creek.



274

275

276 **Figure 6. Overview of the intensive observation period (IOP) from 16 March to 4 April 2024. (a) Air temperature (pink)**
277 **and dew point (blue); (b) wind speed (orange) with wind direction indicated by arrows; (c) cumulative precipitation**
278 **accumulation from the instruments described in the text, including unadjusted Geonor (red), adjusted Geonor (purple),**
279 **adjusted Geonor combined with MRR (blue), and MRR at 35 m (black). Vertical shading denotes observed weather**
280 **conditions: snow (yellow), blowing snow (pink), light precipitation (green), and no precipitation (blue). Unshaded areas**

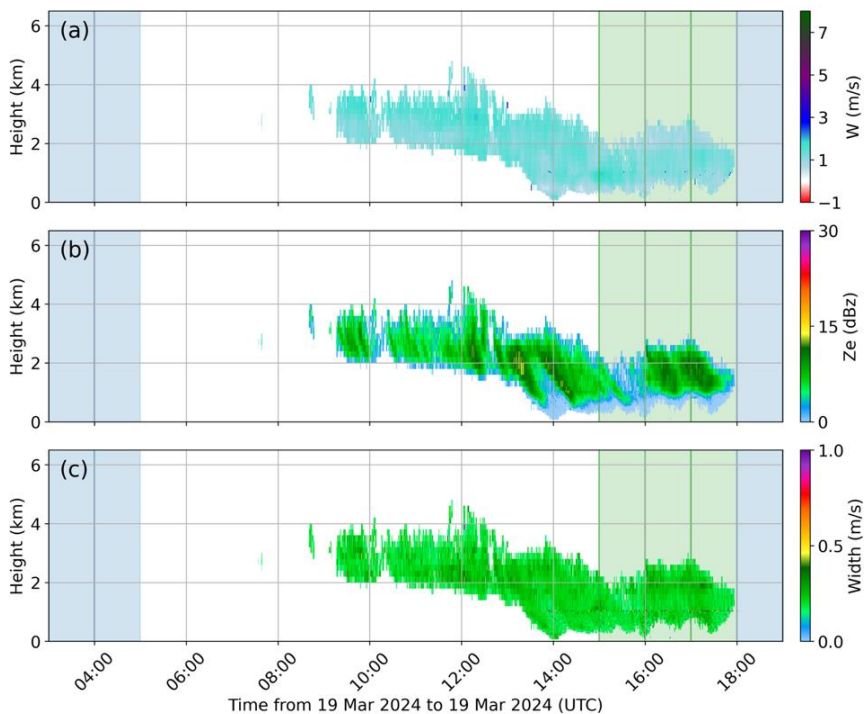
281 **5. Contribution of the light precipitation**

282 Using the manual observations of light precipitation, snow, and no precipitation, we extract the corresponding
283 subset of MRR data to determine precipitation rates and amounts observed during the hourly observations. During
284 the periods of light precipitation and snow that the Geonor did not detect, hourly MRR totals were less than 0.2
285 mm, with a one hour maximum of 0.14 mm. MRR-derived 5 minute precipitation rates during these periods were
286 up to $\sim 1.8 \text{ mm hr}^{-1}$; however, the interquartile range of 5-minute rates from the MRR were $0.03 - 0.3 \text{ mm hr}^{-1}$,
287 with a mean of 0.27 mm hr^{-1} . No discernible signal was detected during periods of no precipitation. An example
288 of vertical profiles obtained from the MRR during the IOP is presented in Fig. 7.

289



290 Despite the extended sensitivity of the MRR, using rate alone to fill in missing precipitation is not suitable due to
 291 the disparity in temporal resolutions between the MRR (5-minute) and the Geonor (hourly). We therefore select
 292 all occurrences during the study period (4 November 2023 – 30 April 2025) where the hourly precipitation amount
 293 recorded by the MRR is between 0.01 and 0.2 mm then exclude hours that the Geonor already detects at least 0.2
 294 mm (i.e., records a non-zero amount). We also amend our working definition of *light precipitation* from this point
 295 onward to match. The total accumulation of light precipitation between 4 November 2023 and 30 April 2024 using
 296 this method is 43 mm, spread over 903 hours. Adding this to the adjusted Geonor increases the total adjusted
 297 accumulation 24% to 215 mm, a 248% increase from the unadjusted amount. We term the combination of these
 298 amounts as *Geonor-MRR adjusted* (Fig. 5). This increases the number of days during the study period that
 299 precipitation was observed from 71 (39% of the study period) to 112 (62%), with 66 days measuring < 1mm (Fig.
 300 8b), a mean daily precipitation amount of 1.91 mm day^{-1} for days with precipitation and 1.20 mm day^{-1} for the
 301 entire study period.

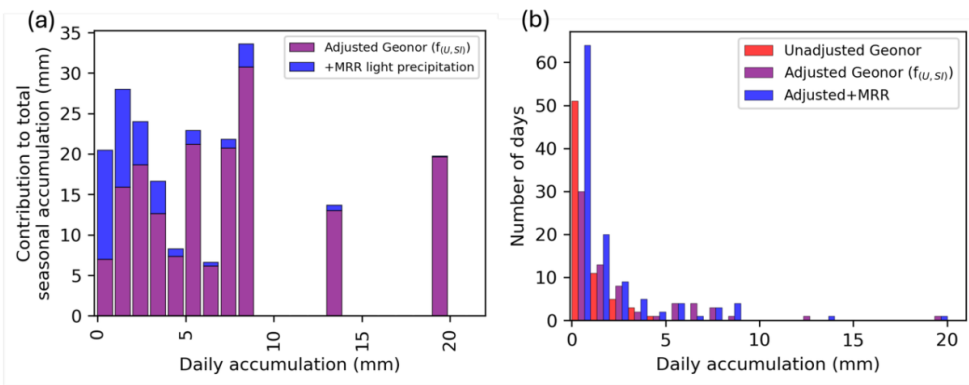


302
 303 **Figure 7.** Time series of MRR profiles for an observed snow event in March. The three panels represent (a) Doppler
 304 velocity of particles (W), (b) effective reflectivity (Ze), and (c) the Doppler spectral width (s). For all profiles, under
 305 1120 m above ground level represents data from the 35 m resolution while above 1120 m are the data from the 200 m
 306 resolution. The background vertical shading corresponds to weather observations: no precipitation observed (blue),
 307 and light precipitation (green). For hours without shading, observations were not available.

308 The largest uncertainty in this method arises from the use of a constant prefactor in Eq. (3), yet Schogger et al.
 309 (2021) illustrate that the largest swing in values for a time-varying a_{zs} , between $500 - 2000 \text{ mm}^{6-bZS} \text{ h}^{bZS} \text{ m}^{-3}$, are
 310 associated with greater amounts of liquid water in the atmosphere, a condition that is unlikely supported at TVC
 311 when light precipitation is observed. We attempt to minimize the error by only employing the MRR adjustment
 312 when necessary (i.e., for periods the Geonor is not sensitive enough) and using a constant a_{zs} appropriate for the



313 conditions. Therefore, the advantage of this method is to add what was confirmed by manual observations to be
314 missing from the Geonor measurements, rather than perform an additional correction or adjustment. The inclusion
315 of MRR derived light precipitation increases the number of days with low precipitation amounts (e.g., 0 – 1 mm,
316 1 – 2 mm), and those days' contribution to the total seasonal accumulation (Fig. 8a).



317
318 **Figure 8. Histograms for total accumulation for Geonor-MRR adjusted accumulation. (a) Number of days for observed**
319 **320 daily accumulation amounts, and (b) total accumulation over 4 November 2023 to 30 April 2024 for observed daily**
accumulation amounts. Histogram bins go from 0.0 mm to 30 mm in 1 mm increments.

321 **6 Concluding Remarks**

322 **6.1 Conclusions**

323 In this study, we have proposed a new method for quantifying the frequent, light precipitation amounts observed
324 at Trail Valley Creek (TVC) research station by adding low-intensity snowfall detected using a micro rain radar
325 (MRR) to the measurements made by a long-running, federally operated Geonor weighing gauge.

326 At TVC, the Geonor gauge records at a minimum hourly resolution of 0.2 mm, which misses low-intensity events.
327 After applying wind and snowfall corrections, recorded totals increased by 204%, underscoring the importance of
328 post-processing. It is unclear, however, whether such corrections are consistently applied by hydrology or ecology
329 users outside the meteorology community.

330 The MRR revealed that light precipitation below the Geonor threshold accounted for ~24% of the seasonal
331 snowpack. Events with intensities of 0.01 – 0.2 mm hr⁻¹ and daily totals <1 mm, though easily overlooked, proved
332 essential to winter accumulation. This demonstrates the importance of small, frequent snowfalls in Arctic
333 environments and highlights the value of complementary manual observations. To bridge these gaps, we used a
334 simple regression model to relate radar reflectivity to snowfall rate. Although less sophisticated than other
335 methods, this approach provides a practical first order estimate and minimizes error by using MRR data only where
336 Geonor records fall short. This strategy is well suited to hydrology focused groups seeking to fill in missing low-
337 rate precipitation within existing networks. The continued operation of these instruments at TVC provides
338 opportunities for refinement, including the use of time-varying regression coefficients, and the fine-tuning of
339 equipment towards finer detection thresholds. Such upgrades would further improve Arctic snowfall measurement
340 and support both scientific and applied uses.



341 **6.2 Limitations**

342 This study reflects a single site and season, limiting its generalizability across Arctic regions. While broader
343 campaigns are common at lower latitudes, reliable data from high latitudes remain scarce, making site-specific
344 results valuable despite this constraint.
345 Geonor measurements consistently underestimate snowfall, and correction factors strongly influence adjusted
346 totals. The coarse hourly resolution and snow/ice buildup on the housing create timing uncertainties relative to
347 higher-resolution radar and disdrometer data. Sublimation and wind-driven advection further complicate the radar–
348 snowfall relationship.
349 The IOP's short duration restricted the range of conditions observed. Heavier snowfall events, such as that of 27
350 December 2023, were missed, precluding evaluation of instrument performance under such conditions. Likewise,
351 limited data on blowing snow prevented analysis of how the instrumentation respond during these periods.

352 **6.3 Implications**

353 Light snowfall, often below the detection limit of conventional gauges, contributes significantly to Arctic
354 snowpack. This finding challenges the adequacy of standard networks and highlights the risk of underestimating
355 water inputs in cold regions.
356 For hydrology, more accurate low-rate snowfall estimates improve snowpack modelling, runoff forecasts, and
357 predictions of streamflow timing – critical for water supply, flood risk, and permafrost stability. For ecology,
358 capturing subtle snowfall inputs refines the understanding of snow-vegetation interactions, soil insulation, and
359 habitat conditions for Arctic species. For climate science, the results provide ground-based evidence that frequent,
360 light snowfall is an important but underrepresented component in Earth system models. Incorporating these
361 processes will improve climate projections in polar regions, where precipitation feedback is key to sea-ice decline,
362 permafrost thaw, and global circulation changes.
363 Finally, this study underscores the importance of communication between disciplines. Hydrologists and ecologists
364 often rely on gauge data but may be unaware of correction requirements or the sensitivity of the instrumentation,
365 leading to systematic underestimation. Improved knowledge exchange between atmospheric scientists and data
366 users will help ensure precipitation records are applied correctly and consistently, strengthening the reliability of
367 Arctic research in support of climate adaptation.



368 **Data availability**

369 Data from the ECCC station at Trail Valley Creek can be found using the ECCC Historical data website,
370 https://climate.weather.gc.ca/historical_data/search_historic_data_e.html (Station name: Trail Valley; Climate ID:
371 220N005). All other data and code used are part of the ongoing *Improved measurements of Arctic snowfall using*
372 *a novel interdisciplinary approach (A-Snow)* project, and currently available by request from the authors. A
373 publicly accessible dataset is planned for the cumulation of the project.

374

375 **Author contributions**

376 PM and JMT designed the study, with input from HDT. HDT deployed the instruments, and HDT and JD
377 participated in the field campaign and data analysis. JD and HDT prepared the manuscript with supervision from
378 JMT and PM. All authors have read and agree to the final version of the published manuscript.

379

380 **Competing interests**

381 The authors declare that they have no conflict of interest.

382

383 **Acknowledgments**

384 This study was conducted under the Northwest Territories Scientific research license #17453, and we thank the
385 Aurora Research Institute in Inuvik, Northwest Territories, for their administrative and logistical support. Many
386 thanks to the staff of the Trail Valley Creek research station for assisting with fieldwork and field logistics.

387

388 **Funding sources**

389 Funding for this research was provided by the Government of Canada's New Frontiers in Research Fund (NFRFE-
390 2022-00669), Canada Research Chairs Program (CRC-2022-00292), and the Natural Sciences and Engineering
391 Research Council of Canada Discovery Grants Program (RGPIN-2019-06654.) Support is also provided from the
392 Canadian Foundation of Innovation's grant for servers and instruments (#37720 and #36146).

393

394



395 **References**

396 Asuma, Y., Iwata, S., Kikuchi, K., Moore, G. W. K., Kimura, R., and Tsuboki, K.: Precipitation Features
397 Observed by Doppler Radar at Tuktoyaktuk, Northwest Territories, Canada, during the Beaufort and Arctic
398 Storms Experiment, *Mon. Wea. Rev.*, 126, 2384–2405, [https://doi.org/10.1175/1520-0493\(1998\)126<2384:PFOBDR>2.0.CO;2](https://doi.org/10.1175/1520-0493(1998)126<2384:PFOBDR>2.0.CO;2), 1998.

400

401 Asuma, Y., Inoue, Y., Kikuchi, K., Kajikawa, M., Sato, N., and Hayasaka, T.: Wintertime precipitation behavior
402 in the western Canadian Arctic region, *Journal of Geophysical Research: Atmospheres*, 105, 14927–14939,
403 <https://doi.org/10.1029/1999JD901124>, 2000.

404

405 Battaglia, A., Rustemeier, E., Tokay, A., Blahak, U., and Simmer, C.: PARSIVEL Snow Observations: A
406 Critical Assessment, *Journal of Atmospheric and Oceanic Technology*, 27, 333–344,
407 <https://doi.org/10.1175/2009JTECHA1332.1>, 2010.

408

409 Brunet, D. and Milbrandt, J. A.: Optimal Design of a Surface Precipitation Network in Canada, *Journal of
410 Hydrometeorology*, 24, 727–742, <https://doi.org/10.1175/JHM-D-22-0085.1>, 2023.

411

412 Chen, L., Voss, C. I., Fortier, D., and McKenzie, J. M.: Surface energy balance of sub-Arctic roads with varying
413 snow regimes and properties in permafrost regions, *Permafrost and Periglacial Processes*, 32, 681–701,
414 <https://doi.org/10.1002/ppp.2129>, 2021.

415

416 Colli, M. and Rasmussen, R.: An Improved Trajectory Model to Evaluate the Collection Performance of Snow
417 Gauges, *Journal of Applied Meteorology and Climatology*, 54, <https://doi.org/10.1175/JAMC-D-15-0035.1>,
418 2015.

419

420 Colli, M., Stagnaro, M., Lanza, L. G., and Rasmussen, R.: Adjustments for Wind-Induced Undercatch in
421 Snowfall Measurements Based on Precipitation Intensity, *Journal of Hydrometeorology*, 21,
422 <https://doi.org/10.1175/JHM-D-19-0222.1>, 2020.

423

424 Environment and Climate Change Canada. Adjusted and homogenized Canadian Climate data. Accessed August
425 17, 2025. Website: <https://www.canada.ca/en/environment-climate-change/services/climate-change/science-research-data/climate-trends-variability/adjusted-homogenized-canadian-data.html>. 2023.

427

428 Gultepe, I., Rabin, R., Ware, R., and Pavolonis, M.: Light Snow Precipitation and Effects on Weather and
429 Climate, in: *Advances in Geophysics*, vol. 57, Elsevier, 147–210, <https://doi.org/10.1016/bs.agph.2016.09.001>,
430 2016.

431

432 HydroMet OTT: Operating instructions present weather sensor OTT parsivel 2, 2016.

433

434 Jitnikovitch, A., Marsh, P., Walker, B., and Desilets, D.: Snow water equivalent measurement in the Arctic based
435 on cosmic ray neutron attenuation. *Cryosphere*, 15(11), 5227–5239. <https://doi.org/10.5194/tc-15-5227-2021>,
436 2021.

437

438 Kochendorfer, J., Earle, M., Rasmussen, R., Smith, C., Yang, D., Morin, S., Mekis, E., Buisan, S., Roulet, Y.-A.,
439 Landolt, S., Wolff, M., Hoover, J., Thériault, J. M., Lee, G., Baker, B., Nitu, R., Lanza, L., Colli, M., and
440 Meyers, T.: How Well Are We Measuring Snow Post-SPICE?, *Bulletin of the American Meteorological Society*,
441 103, E370–E388, <https://doi.org/10.1175/BAMS-D-20-0228.1>, 2022.

442

443 Kochendorfer, J., Nitu, R., Wolff, M., Mekis, E., Rasmussen, R., Baker, B., Earle, M., Reverdin, A., Wong, K.,
444 Smith, C. D., Yang, D., Roulet, Y. A., Meyers, T., Buisan, S., Isaksen, K., Brækkan, R., Landolt, S., & Jachcik,
445 A.: Testing and development of transfer functions for weighing precipitation gauges in WMO-SPICE.
446 *Hydrology and Earth System Sciences*, 22(2), 1437–1452. <https://doi.org/10.5194/hess-22-1437-2018>, 2018.



447 Kochendorfer, J., Rasmussen, R., Wolff, M., Baker, B., Hall, M. E., Meyers, T., Landolt, S., Jachcik, A.,
448 Isaksen, K., Brækkan, R., & Leeper, R.: The quantification and correction of wind-induced precipitation
449 measurement errors. *Hydrology and Earth System Sciences*, 21(4), 1973–1989. <https://doi.org/10.5194/hess-21-1973-2017>, 2017.

450

451 Leroux, N. R., Thériault, J. M., and Rasmussen, R.: Improvement of Snow Gauge Collection Efficiency through
452 a Knowledge of Solid Precipitation Fall Speed, *Journal of Hydrometeorology*, 22, 997–1006,
453 <https://doi.org/10.1175/JHM-D-20-0147.1>, 2021.

454

455 Maahn, M. and Kollias, P.: Improved Micro Rain Radar snow measurements using Doppler spectra post-
456 processing, *Atmos. Meas. Tech.*, 5, 2661–2673, <https://doi.org/10.5194/amt-5-2661-2012>, 2012.

457

458 Marsh, P., Mann, P., & Walker, B.: Changing snowfall and snow cover in the western Canadian Arctic. In W.
459 Quinton (Ed.), 22nd Northern Research Basins Symposium and Workshop (pp. 1–10).
460 <https://conferences.wlu.ca/22ndnrb/>, 2019.

461

462 Marsh, P., Onclin, C., & Russell, M. A. R. K.: A multi-year hydrological data set for two research basins in the
463 Mackenzie Delta region, NW Canada. In D. Kane & D. Yang (Eds.), *Northern Research Basins Water Balance*.
464 Proceedings of a Workshop. IAHS Publ. 290 (Issue IAHS Publication 290, pp. 205–212). International
465 Association of Hydrological Sciences, 2004

466

467 Marsh, P., & Pomeroy, J. W: Meltwater fluxes at an arctic forest-tundra site. *Hydrological Processes*, 10(10),
468 1383–1400. [https://doi.org/10.1002/\(SICI\)1099-1085\(199610\)10:10<1383::AID-HYP468>3.0.CO;2-W](https://doi.org/10.1002/(SICI)1099-1085(199610)10:10<1383::AID-HYP468>3.0.CO;2-W), 1996.

469

470

471 Mariani, Z., Burrows, W. R., Gascon, G., & Crawford, R.: A Machine-Learning Method to Integrate Arctic
472 Supersite Observations and Diagnose Weather Element Occurrence. *Atmosphere-Ocean*, 62(2), 119–134.
473 <https://doi.org/10.1080/07055900.2023.2257651>, 2024

474

475 Mariani, Z., Huang, L., Crawford, R., Blanchet, J. P., Hicks-Jalali, S., Mekis, E., Pelletier, L., Rodriguez, P., and
476 Strawbridge, K.: Enhanced automated meteorological observations at the Canadian Arctic Weather Science
477 (CAWS) supersites. *Earth System Science Data*, 14(11), 4995–5017. <https://doi.org/10.5194/essd-14-4995-2022>,
478 2022.

479

480 Matrosov, S. Y., Shupe, M. D., and Uttal, T.: High temporal resolution estimates of Arctic snowfall rates
481 emphasizing gauge and radar-based retrievals from the MOSAiC expedition. *Elementa*, 10(1).
482 <https://doi.org/10.1525/elementa.2021.00101>, 2022

483

484 Metek, M. M. G.: MRR-2: Micro rain radar, User manual, 2009.

485

486 Meloche, J., Langlois, A., Rutter, N., Royer, A., King, J., Walker, B., Marsh, P., and Wilcox, E. J.:
487 Characterizing tundra snow sub-pixel variability to improve brightness temperature estimation in satellite SWE
488 retrievals, *The Cryosphere*, 16, 87–101, <https://doi.org/10.5194/tc-16-87-2022>, 2022.

489

490 Morse, P.D., Burn, C.R., and Kokelj, S.V.: Influence of snow on near-surface ground temperatures in upland and
491 alluvial environments of the outer Mackenzie Delta, Northwest Territories. *Canadian Journal of Earth Sciences*.
492 49(8): 895–913. <https://doi.org/10.1139/e2012-012>, 2012.

493

494 O'Neill, H. B. and Burn, C. R.: Impacts of variations in snow cover on permafrost stability, including simulated
495 snow management, Dempster Highway, Peel Plateau, Northwest Territories, *Arctic Science*, 3, 150–178,
496 <https://doi.org/10.1139/as-2016-0036>, 2017.

497



498 Pierre, A., Jutras, S., Smith, C., Kochendorfer, J., Fortin, V., & Anctil, F.: Evaluation of catch efficiency transfer
499 functions for unshielded and single-alter-shielded solid precipitation measurements. *Journal of Atmospheric and*
500 *Oceanic Technology*, 36(5), 865–881. <https://doi.org/10.1175/JTECH-D-18-0112.1>, 2019.

501

502 Previdi, M., Smith, K. L., and Polvani, L. M.: Arctic amplification of climate change: a review of underlying
503 mechanisms, *Environ. Res. Lett.*, 16, 093003, <https://doi.org/10.1088/1748-9326/ac1c29>, 2021.

504

505 Przybylak, R.: Variability of total and solid precipitation in the Canadian Arctic from 1950 to 1995, *Intl Journal*
506 *of Climatology*, 22, 395–420, <https://doi.org/10.1002/joc.750>, 2002.

507

508 Rasmussen, R., Baker, B., Kochendorfer, J., Meyers, T., Landolt, S., Fischer, A. P., Black, J., Thériault, J. M.,
509 Kucera, P., Gochis, D., Smith, C., Nitu, R., Hall, M., Ikeda, K., and Gutmann, E.: How Well Are We Measuring
510 Snow: The NOAA/FAA/NCAR Winter Precipitation Test Bed, *Bulletin of the American Meteorological*
511 *Society*, 93, 811–829, <https://doi.org/10.1175/BAMS-D-11-00052.1>, 2012.

512

513 Rasmussen, R., Dixon, M., Vasiloff, S., Hage, F., Knight, S., Vivekanandan, J., & Xu, M.: Snow Nowcasting
514 Using a Real-Time Correlation of Radar Reflectivity with Snow Gauge Accumulation. *Journal of Applied*
515 *Meteorology*, 42(1), 20–36. [https://doi.org/10.1175/1520-0450\(2003\)042<0020:SNUART>2.0.CO;2](https://doi.org/10.1175/1520-0450(2003)042<0020:SNUART>2.0.CO;2), 2003

516

517 Schoger, S. Y., Moisseev, D., Von Lerber, A., Crewell, S., and Eboll, K.: Snowfall-Rate Retrieval for K- and W-
518 Band Radar Measurements Designed in Hyttiälä, Finland, and Tested at Ny-Ålesund, Svalbard, Norway, *Journal*
519 *of Applied Meteorology and Climatology*, 60, 273–289, <https://doi.org/10.1175/JAMC-D-20-0095.1>, 2021.

520

521 Smith, C. D., Ross, A., Kochendorfer, J., Earle, M. E., Wolff, M., Buisán, S., Roulet, Y.-A., and Laine, T.:
522 Evaluation of the WMO Solid Precipitation Intercomparison Experiment (SPICE) transfer functions for
523 adjusting the wind bias in solid precipitation measurements, *Hydrology and Earth System Sciences*, 24, 4025–
524 4043, <https://doi.org/10.5194/hess-24-4025-2020>, 2020.

525

526 Souverijns, N.: Estimating radar reflectivity - Snowfall rate relationships and their uncertainties over Antarctica
527 by combining disdrometer and radar observations, *Atmospheric Research*,
528 <https://doi.org/10.1016/j.atmosres.2017.06.001>, 2017.

529

530 Thériault, J. M., Déry, S. J., Pomeroy, J. W., Smith, H. M., Almonte, J., Bertoncini, A., Crawford, R. W.,
531 Desroches-Lapointe, A., Lachapelle, M., Mariani, Z., Mitchell, S., Morris, J. E., Hébert-Pinard, C., Rodriguez,
532 P., & Thompson, H. D.: Meteorological observations collected during the Storms and Precipitation Across the
533 continental Divide Experiment (SPADEF), April–June 2019. *Earth System Science Data*, 13(3), 1233–1249.
534 <https://doi.org/10.5194/essd-13-1233-2021>, 2021.

535

536 Thériault, J. M., Leroux, N. R., & Rasmussen, R. M.: Improvement of solid precipitation measurements using a
537 hotplate precipitation gauge. *Journal of Hydrometeorology*, 22(4), 877–885. <https://doi.org/10.1175/JHM-D-20-0168.1>, 2021.

539

540 Thompson, H. D., Thériault, J. M., Déry, S. J., Stewart, R. E., Boisvert, D., Rickard, L., Leroux, N. R., Colli, M.,
541 & Vionnet, V.: Atmospheric and surface observations during the Saint John River Experiment on Cold Season
542 Storms (SAJESS). *Earth System Science Data*, 15(12), 5785–5806. <https://doi.org/10.5194/essd-15-5785-2023>,
543 2023.

544

545 von Lerber, A., Moisseev, D., Bliven, L. F., Petersen, W., Harri, A.-M., & Chandrasekar, V.: Microphysical
546 Properties of Snow and Their Link to Ze–S Relations during BAECC 2014. *Journal of Applied Meteorology and*
547 *Climatology*, 56(6), 1561–1582. <https://doi.org/10.1175/JAMC-D-16-0379.1>, 2017.

548

549 Walker, B. J. and Marsh, P.: High resolution spatial variability in spring snowmelt for an Arctic shrub-tundra
550 watershed, <https://doi.org/10.13140/RG.2.2.16836.78728>, 2019.



551 Wilcox, E. J., Wolfe, B. B., & Marsh, P.: Hydrological, meteorological, and watershed controls on the water
552 balance of thermokarst lakes between Inuvik and Tuktoyaktuk, Northwest Territories, Canada. *Hydrology and*
553 *Earth System Sciences*, 27(11), 2173–2188. <https://doi.org/10.5194/hess-27-2173-2023>, 2023.

554

555 Woo, M. K., Heron, R., Marsh, P., & Steer, P. (1983). Comparison of weather station snowfall with winter snow
556 accumulation in High Arctic basins. *Atmosphere-Ocean*, 21(3), 312–325.

557 World Meteorological Organization: Guide des instruments et des méthodes d'observation:
558 <https://library.wmo.int/records/item/68681-guide-des-instruments-et-des-methodes-d-observation>, last access: 28
559 May 2024.

560

561 Yuter, S. E., Kingsmill, D. E., Nance, L. B., & Löffler-Mang, M.: Observations of Precipitation Size and Fall
562 Speed Characteristics within Coexisting Rain and Wet Snow. *Journal of Applied Meteorology and Climatology*,
563 45(10), 1450–1464. <https://doi.org/10.1175/JAM2406.1>, 2006.

564